ARTICLE

Infrared Photodissociation Spectroscopic and Theoretical Study of [Co(CO$_2$)$_n$]$^+$ Clusters†

Dong Yang[a,b‡], Ming-zhi Su[a,b‡], Hui-jun Zheng[a,b], Zhi Zhao[a], Gang Li[a], Xiang-tao Kong[a], Hua Xie[a], Hong-jun Fan[a], Wei-qing Zhang[a], Ling Jiang[a*]

a. State Key Laboratory of Molecular Reaction Dynamics, Collaborative Innovation Center of Chemistry for Energy and Materials, Dalian Institute of Chemical Physics, Chinese Academy of Sciences, Dalian 116023, China
b. University of Chinese Academy of Sciences, Beijing 100049, China

The mass-selected infrared photodissociation (IRPD) spectroscopy was utilized to investigate the interactions of cationic cobalt with carbon dioxide molecules. Quantum chemical calculations were performed on the [Co(CO$_2$)$_n$]$^+$ clusters to identify the structures of the low-lying isomers and to assign the observed spectral features. All the [Co(CO$_2$)$_n$]$^+$ ($n=2-6$) clusters studied here show resonances near the CO$_2$ asymmetric stretch of free CO$_2$ molecule. Experimental and calculated results indicate that the CO$_2$ molecules are weakly bound to the Co$^+$ cations in an end-on configuration via a charge-quadrupole electrostatic interaction. The present IRPD spectra of [Co(CO$_2$)$_n$]$^+$ clusters have been compared to those of Ar-tagged species ([Co(CO$_2$)$_n$]$^+$-Ar), which would provide insights into the tagging effect of rare gas on the weakly-bounded clusters.

Key words: Cationic cobalt, Carbon dioxide, Structure, Infrared photodissociation spectroscopy, Quantum chemical calculation

I. INTRODUCTION

The transformation of carbon dioxide CO$_2$ in chemistry continues to be a subject of intensive investigation because of the double-faced property of CO$_2$, a primary cause to global warming and an abundant renewable resource for the production of fine chemicals and clean fuels [1–3]. Metal complexes are widely involved in the catalytic activation of CO$_2$ molecule [4, 5]. In particular, extensive theoretical and experimental studies have been performed with particular focus on the transition metal catalyst. Modern laboratory-based intense, tunable infrared systems and spectroscopy afford a fundamental insight into the reaction on the carbon dioxide with ions, which provide detailed information for mechanistic understanding at the molecular level [6–11].

Cluster spectroscopy and quantum chemical calculations have been utilized to investigate the interaction of carbon dioxide with neutral, cationic, and anionic metal atoms in the gas phase [12–15]. In the neutral complexes, monodentate coordination M(η^1-CO$_2$), bidentate coordination M(η^2-CO$_2$), or inserted OMCO

structures have been observed [12, 16, 17]. For the reactions of CO$_2$ with metal anions, monodentate coordination [M(η^1-CO$_2$)]$^-$ has been characterized for M=Bi$^-$, Cu$^-$, Ag$^-$, Au$^-$ anions [18–21], and the bidentate configuration [M(η^2-CO$_2$)]$^-$ for Co$^-$ and Ni$^-$ [22, 23]. A bidentate complexe [ClMg(η^2-O$_2$C)]$^-$ has also been identified [24].

Generally, the M$^+$-OCO configuration is common in the cation-CO$_2$ complexes. The metal cations bind to the oxygen atom of CO$_2$ in an end-on configuration as a result of charge-quadrupole electrostatic interaction [25–31]. However, for the larger [M(CO$_2$)$_n$]$^+$ (M=Ti, Ni, Si; $n \geq 5$) complexes, the spectra provide evidence for an intracluster insertion reaction that produces a metal oxide-carbonyl [OMCO(CO$_2$)$_{n-1}$]$^+$ species [28–30]. The oxalate-type [V(C$_2$O$_4$)(CO$_2$)$_5$]$^+$ species has been proposed in the interactions of vanadium cations with carbon dioxide molecules [31]. Recently, infrared photodissociation (IRPD) spectroscopic study of rare gas-tagged [M(CO$_2$)$_n$]$^+$-Ar (M=Co, Rh, Ir; $n=2-15$) clusters suggested the formation of a core [M(CO$_2$)$_2$]$^+$ structure, to which the subsequent ligands are less strongly bound [32]. In this work, we report the IRPD spectra of untagged [Co(CO$_2$)$_n$]$^+$ clusters, in which structural assignment is aided by density functional calculations. The combination of experimental and calculated IR spectra of [Co(CO$_2$)$_n$]$^+$ ($n=2-6$) reveals that the CO$_2$ molecules are weakly bound to the Co$^+$ cations in an end-on configuration via a charge-quadrupole elec-

---

II. EXPERIMENTAL METHOD

The experiments were carried out on an IRPD instrument, which has been described in detail in our previous work [33]. Briefly, the experimental setup consisted of a laser vaporization supersonic cluster source, a tandem time-of-flight (TOF) mass spectrometer, and a tunable infrared laser source. The 532 nm output of a Nd:YAG laser was focused on vaporizing the rotating metal target. The purities of the target was higher than 99.9%, and the surface of the target was polished prior to the experiments to ensure a clean vaporization target. The $[Co(CO_2)_n]^+$ complexes were produced by the reactions of the vaporized species with CO_2. The stagnation pressure of the reaction gas was approximately $5-8$ atm and the gas was introduced into the vacuum region through a pulsed valve (General Valve, series 9). After free expansion, all products were skimmed into the acceleration region and analyzed using the first stage of the TOF system. The cations of interest were mass-selected and decelerated into the extraction region of the vertical second stage of the TOF system. Here, a pulsed infrared laser was irradiated to the selected cationic packet in the acceleration region of the vertical second stage TOF mass spectrometer, which analyzed the dissociation fragments and the remaining parent cations. Typical spectra were recorded by scanning the infrared laser in the step size of 2 cm^{-1}. IRPD spectra were obtained by recording the fragment cations as a function of the tunable IR laser wavelength.

The tunable infrared laser beam was generated by a KTP/KTA optical parametric oscillator/amplifier system (OPO/OPA, LaserVision) pumped by an injection-seeded Nd:YAG laser (Continuum Surelite EX). The system provided tunable IR output radiation from 700 cm^{-1} to 7000 cm^{-1} with a line width of 1 cm^{-1}. The wavelength of the OPO laser output was calibrated using a commercial wavelength meter (Bristol, 821 Pulse Laser Wavelength Meter).

III. COMPUTATIONAL METHOD

Quantum chemical calculations were carried out to study the structures, bonding, and vibrational spectra of $[Co(CO_2)_n]^+$ using the Gaussian 09 package [34]. The structures were optimized by B3LYP hybrid functionals augmented with a dispersion correction (B3LYP-D) together with the 6-311+G(d,p) basis set for all elements. The integral grid used for the calculations was a pruned (99 590) grid (the "ultrafine" grid as defined by Gaussian 09). Relative energies and binding energies included zero-point vibrational energies. The harmonic vibrational frequencies were scaled by a factor of 0.964, which was determined by the ratio of the
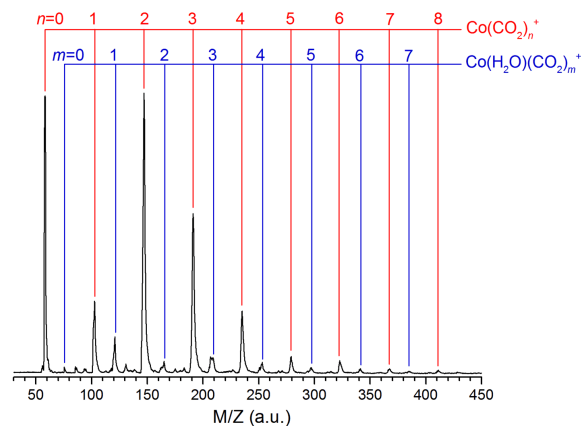

FIG. 1 Mass spectra of the $[Co(CO_2)_n]^+$ ($n=1-8$) cluster ions (indicated in red) produced by pulsed laser vaporization of cobalt metal targets in a supersonic expansion of CO_2. The mass spectra of the $[Co(H_2O)(CO_2)_m]^+$ ($m=1-7$) complexes (indicated in blue) are also included for comparision.

experimental value (2349 cm^{-1}) to the B3LYP-D calculated one (2437 cm^{-1}) of free CO_2 molecule. The resulting stick spectra were convoluted by a Gaussian line shape function with a full width at half maximum line width of 6 cm^{-1}, in order to account for line-broadening effects.

All of the energy minima have been verified by vibrational frequency calculations. We checked the ground state multiplicities for the lowest-energy isomers and those with close energies. The triplet state was the lowest in energies for all of the structures.

IV. RESULTS AND DISCUSSION

A. Experimental results

The mass spectra of the $[Co(CO_2)_n]^+$ clusters are shown in FIG. 1. The major signals are dominated by the $[Co(CO_2)_n]^+$ ($n=1-8$) ions. The similar situations appear in the reactions of CO_2 with Fe^+, Ni^+, Cu^+, and Ag^+ cations [26, 28, 35]. The mass-selected $[Co(CO_2)_n]^+$ clusters were introduced into the infrared photodissociation region. The cations absorbed IR photons and fragmented when the vibration of the cation was resonant with the tunable IR laser frequency. The lowest dissociation energy of $n=1$ was calculated to be 97.8 kJ/mol at the B3LYP-D3/6-311+G(d,p) level of theory (Table I). Assuming that the internally cold $[Co(CO_2)]^+$ is formed, the absorption of at least four photons around 2350 cm^{-1} is required to overcome the dissociation limit. The single pass of photon fluence generated from the table-top LaserVision system might be insufficient to induce photofragmentation of $[Co(CO_2)]^+$ under the present experimental conditions. Beginning at the $n=2$ cluster, the fragmentation was

TABLE I Lowest dissociation energies (E_{diss}) for the loss of one CO_2 molecule for $[Co(CO_2)_n]^+$ ($n=1-6$) at the B3LYP-D3/6-311+G(d,p) level and the number N of IR photon required to overcome the dissociation limit at 2350 cm^{-1}.

n	E_{diss}/(kJ/mol)	N
1	97.8	4
2	89.6	4
3	50.0	2
4	40.6	2
5	36.3	2
6	31.3	2
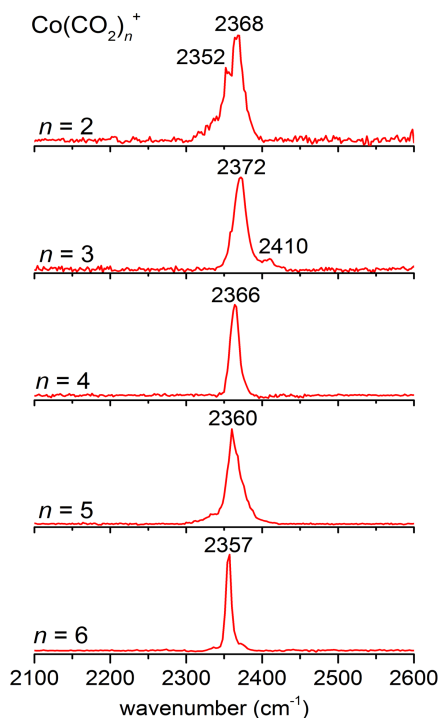
FIG. 2 Experimental IRPD spectra in the CO_2 asymmetric stretch region of $[Co(CO_2)_n]^+$ ($n=2-6$).
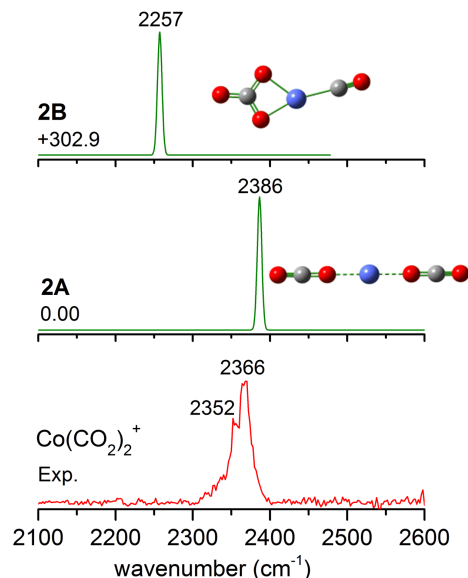

FIG. 3 Optimized structures (Co: blue, C: gray, O: red) together with the experimental IRPD spectra (indicated in red) and simulated harmonic IR spectra (indicated in green) of $[Co(CO_2)_2]^+$ isomers calculated at the B3LYP-D/6-311+G(d,p) level. Relative energies (with ZPE correction) are given in kJ/mol.

observed. Higher fragmentation yield was obtained for the $n=3-6$ clusters. The number densities of $n=7$ and 8 were insufficient for the obvious detection of fragmentation. The IRPD spectra of $[Co(CO_2)_n]^+$ ($n=2-6$) have been measured experimentally, which are shown in FIG. 2.

The principal features in the IRPD spectra of $[Co(CO_2)_n]^+$ ($n=2-6$) clusters are observed at 2368, 2352, 2366, 2360, and 2357 cm^{-1}, respectively. These band positions are characteristic of the antisymmetric stretch of CO_2. As illustrated in FIG. 2, two bands are observed for $[Co(CO_2)_n]^+$ ($n=2$ and 3) and the relative intensity of the satellite peaks decrease with increasing cluster size. The IRPD spectra of $[Co(CO_2)_n]^+$ ($n=4-6$) exhibits a single strong absorption respectively. This is different from the IRPD spec-

tra of rare gas-tagged $[Co(CO_2)_n]^+$-Ar clusters [32]. The $[Co(CO_2)_2]^+$-Ar gave a single strong feature at 2385 cm^{-1} and $[Co(CO_2)_n]^+$-Ar ($n \geq 3$) yielded two bands, in which the primary bands of 2385 cm^{-1} were assigned to the $[Co(CO_2)_2]^+$ core, and the additional vibrational bands were ascribed to the more weakly bound CO_2 ligands [32].

B. Comparison of experimental and theoretical results

For each cluster of $n=2-6$, the structures, energetics, and simulated IR spectra of the isomers are shown together with the corresponding experimental IRPD spectra in FIGs. 3−7, respectively.

In FIG. 3, the lowest-lying structure of $[Co(CO_2)_2]^+$ cluster (labeled 2A) has an end-on linear configuration with the two CO_2 molecules terminally bonded to the Co cation. The next energetically higher isomer (2B, +302.9 kJ/mol) consists of a bidentate double oxygen metal-CO_3 and a terminal CO. The CO_2 antisymmetric stretching vibrational frequency in the 2A isomer is calculated to be 2386 cm^{-1}, which is in agreement with the main experimental feature of 2368 cm^{-1}. In the simulated IR spectrum of isomer 2B, a strong absorption observed at 2257 cm^{-1} is assigned to the C−O stretch, which is absent from the experimental spectrum. The 2A isomer should contribute to the experimental spectrum of $n=2$.

As shown in FIG. 4, the lowest-energy isomer (3A) for $[Co(CO_2)_3]^+$ cluster has three terminally bonded CO_2 molecules. The 3B isomer contains a
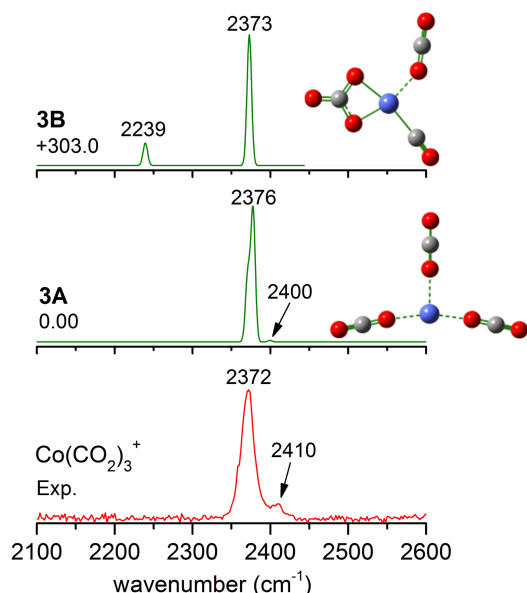

FIG. 4 Optimized structures (Co: blue, C: gray, O: red) together with the experimental IRPD spectra (indicated in red) and simulated harmonic IR spectra (indicated in green) of $[\text{Co}(CO_2)_3]^+$ isomers calculated at the B3LYP-D/6-311+G(d,p) level. Relative energies (with ZPE correction) are given in kJ/mol.

FIG. 5 Optimized structures (Co: blue, C: gray, O: red) together with the experimental IRPD spectra (indicated in red) and simulated harmonic IR spectra (indicated in green) of $[\text{Co}(CO_2)_4]^+$ isomers calculated at the B3LYP-D/6-311+G(d,p) level. Relative energies (with ZPE correction) are given in kJ/mol.

$[(OC)Co(CO_3)(CO_2)]^+$ carbonyl-carbonate structure, which lies 303.0 kJ/mol higher in energy than 3A. The strong absorption at 2376 cm^{-1} and the satellite peak at 2400 cm^{-1} for 3A match well with the experimental features of 2372 cm^{-1} and 2410 cm^{-1} (FIG. 4). In the calculated IR spectrum of 3B, the frequencies at 2239 and 2373 cm^{-1} are attributed to the C−O stretch and CO_2 antisymmetric stretch, respectively, of which the former is also not observed in the experiment. It thus appears that isomer 3A is responsible for the experimental IRPD spectrum of $[\text{Co}(CO_2)_3]^+$, whereas isomer 3B can be ruled out.

FIG. 5 shows the results of $[\text{Co}(CO_2)_4]^+$. The lowest-energy isomer is a D_{4h} symmetrical structure (4A) with four ligands coordinated directly to the metal. The $[(OC)Co(CO_3)(CO_2)_2]^+$ carbonyl-carbonate structure (4B) lies 246.6 kJ/mol higher in energy than 4A. The CO_2 antisymmetric stretch is predicted at 2370 cm^{-1} in the simulated IR spectrum of isomer 4A (FIG. 5), which is consistent with the experiment value of 2366 cm^{-1}. The calculated IR spectrum of isomer 4B yields the obvious splitting of the CO_2 antisymmetric stretches at 2360 cm^{-1} and 2373 cm^{-1}, whose feature is absent from the experimental spectrum, as well as the predicted C−O stretch at 2238 cm^{-1}. For n=4 cluster, isomer 4B can be excluded on the basis of the absence of the C−O stretch and the splitting feature of CO_2 antisymmetric stretches from the experiment.

For $[\text{Co}(CO_2)_5]^+$, the lowest-energy isomer (5A) is predicted to be a five-coordinated structure (FIG. 6). The energetically higher isomer 5B (+250.2 kJ/mol) has
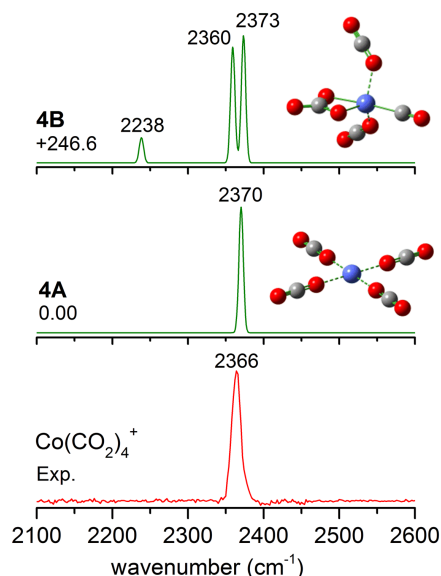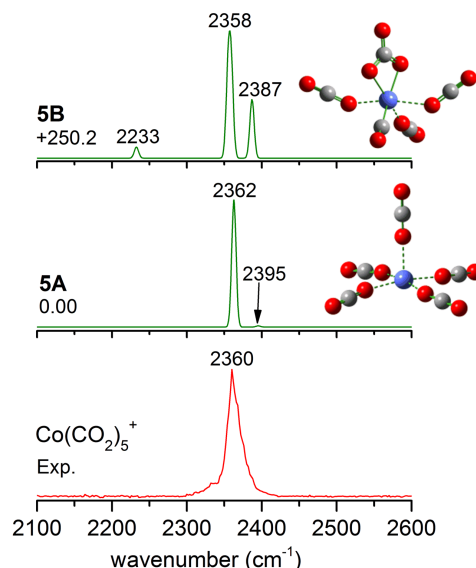

FIG. 6 Optimized structures (Co: blue, C: gray O: red) together with the experimental IRPD spectra (indicated in red) and simulated harmonic IR spectra (indicated in green) of $[\text{Co}(CO_2)_5]^+$ isomers calculated at the B3LYP-D/6-311+G(d,p) level. Relative energies (with ZPE correction) are given in kJ/mol.

a $[(OC)Co(CO_3)(CO_2)_3]^+$ carbonyl-carbonate structure. It can be seen from FIG. 6 that the simulated IR spectrum of 5A agrees with experiment. In the simulated IR spectrum of 5B, the C−O stretch (2233 cm^{-1}) is not present in the experimental IRPD spectrum, as well as the splitting feature of CO_2 antisymmetric
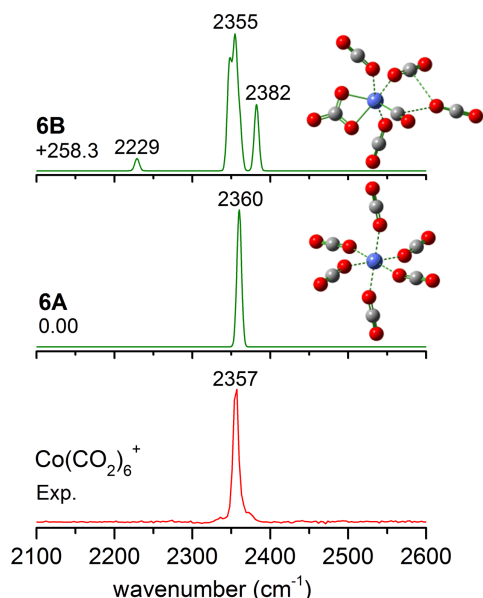
FIG. 7 Optimized structures (Co: blue, C: gray, O: red) together with the experimental IRPD spectra (indicated in red) and simulated harmonic IR spectra (indicated in green) of $[Co(CO_2)_6]^+$ isomers calculated at the B3LYP-D/6-311+G(d,p) level. Relative energies (with ZPE correction) are given in kJ/mol.

stretches (2358 and 2387 cm^{-1}). The 5A isomer should contribute to the experimental spectrum of n=5 instead of 5B.

As shown in FIG. 7, the lowest-energy isomer (6A) of $[Co(CO_2)_6]^+$ cluster has the six CO_2 molecules terminally bonded structure. The $[(OC)Co(CO_3)(CO_2)_4]^+$ carbonyl-carbonate structure 6B with an external CO_2 is calculated to be +258.3 kJ/mol higher in energy above 6A. The calculated IR spectra of 6A give an intense peak at 2360 cm^{-1}, which reproduces well the experimental feature. The 6B isomer yields a broader band centered at 2355 cm^{-1} and an adjacent peak at 2382 cm^{-1}, whereas the latter is not observed in the experiment. Then, isomer 6A is responsible for the experimental IRPD spectrum of $[Co(CO_2)_6]^+$. The explanations for the much narrower bandwidth observed for the n=6 cluster include the higher photodissociation efficiency benefiting from the smaller dissociation energy (Table I) and the highly symmetric geometry.

C. Structural evolution

It can be seen from the above analysis that present calculations for $[Co(CO_2)_n]^+$ (n=2−6) yielded two types of structures for each cluster. The first type is where the CO_2 molecules are weakly bonded to the Co cation in an end-on linear configuration (labeled nA). The second type is the $[(CO)Co(CO_3)(CO_2)_{n-2}]^+$ carbonyl-carbonate struc-

ture (labeled nB). For $[Co(CO_2)_n]^+$ (n=2−6), the formation of nA structure is energetically favored, whereas that of carbonyl-carbonate structures (nB) is not dominated. Furthermore, the calculated IR spectra of the nA isomers are in agreement with the experimental ones, whereas those of the nB isomers are discrepant from the experimental ones. It thus can be concluded that the Co$^+$ cations bind to an oxygen atom of CO_2 in an end-on configuration interaction and the formation of carbonyl-carbonate structures is not favored for the interaction of CO_2 with Co$^+$. The present finding is different from the previous IRPD spectroscopic study of rare gas-tagged $[Co(CO_2)_n]^+$-Ar clusters with preferential formation of a core $[Co(CO_2)_2]^+$ structure [32]. This indicates that the tagging of rare gas to the $[Co(CO_2)_n]^+$ cluster is not innocent, but makes an obvious effect on the vibrational profiles. The reason could be due to that the rare gas remarkably affects the energetic landscape of the weakly-bounded clusters.

The structural features of $[Co(CO_2)_n]^+$ clusters observed here are reminiscent of of $[M(CO_2)_n]^+$ (M=Mg, Al, Si, Fe, Ni, Cu, and Ag) [25–31, 35]. The blue-shift of antisymmetric stretch of CO_2 in these $[M(CO_2)_n]^+$ clusters from the free CO_2 molecules at 2349 cm^{-1} decreases with the increase of cluster size, which is due to the coordination of more weakly bound ligands.

V. CONCLUSION

Mass-selected infrared photodissociation spectroscopy combined with quantum chemical calculation was used to study the interactions of cobalt cations with carbon dioxide molecules. The $[Co(CO_2)_n]^+$ clusters were obtained by the laser vaporization supersonic cluster source and irradiated with infrared laser after mass selection. The results indicated that the Co$^+$ ions bind to an oxygen atom of CO_2 in an end-on configuration by a charge-quadrupole electrostatic interaction. For $[Co(CO_2)_n]^+$ (n=2−6), the carbonyl-carbonate structures is not favored in energy. The comparison of IRPD spectra of $[Co(CO_2)_n]^+$ clusters with those of Ar-tagged species ($[Co(CO_2)_n]^+$-Ar) is discussed.

VI. ACKNOWLEDGEMENTS

[1] D. H. Gibson, Chem. Rev. **96**, 2063 (1996).

[2] T. Sakakura, J. C. Choi, and H. Yasuda, Chem. Rev. **107**, 2365 (2007).

[3] W. Taifan, J. F. Boily, and J. Baltrusaitis, Surf. Sci. Rep. **71**, 595 (2016).

[4] M. North, R. Pasquale, and C. Young, Green Chem. **12**, 1514 (2010).

[5] X. B. Lu and D. J. Darensbourg, Chem. Soc. Rev. **41**, 1462 (2012).

[6] A. W. Castleman and R. G. Keesee, Acc. Chem. Res. **19**, 413 (1986).

[7] Z. Luo, A. W. Castleman Jr., and S. N. Khanna, Chem. Rev. **116**, 14456 (2016).

[8] D. K. Bohme and H. Schwarz, Angew. Chem. Int. Ed. **44**, 2336 (2005).

[9] C. J. Weinheimer and J. M. Lisy, J. Chem. Phys. **105**, 2938 (1996).

[10] C. J. Weinheimer and J. M. Lisy, J. Phys. Chem. **100**, 15305 (1996).

[11] J. M. Lisy, Int. Rev. Phys. Chem. **16**, 267 (1997).

[12] J. Mascetti, F. Galan, and I. Papai, Coord. Chem. Rev. **190**, 557 (1999).

[13] N. R. Walker, R. S. Walters, and M. A. Duncan, New J. Chem. **29**, 1495 (2005).

[14] J. M. Weber, Int. Rev. Phys. Chem. **33**, 489 (2014).

[15] H. Schwarz, Coord. Chem. Rev. **334**, 112 (2017).

[16] M. F. Zhou and L. Andrews, J. Am. Chem. Soc. **120**, 13230 (1998).

[17] L. Jiang and Q. Xu, J. Phys. Chem. A **111**, 3519 (2007).

[18] M. C. Thompson, J. Ramsay, and J. M. Weber, Angew. Chem. Int. Ed. **55**, 15171 (2016).

[19] B. J. Knurr and J. M. Weber, J. Phys. Chem. A **118**, 10246 (2014).

[20] B. J. Knurr and J. M. Weber, J. Phys. Chem. A **117**, 10764 (2013).

[21] B. J. Knurr and J. M. Weber, J. Am. Chem. Soc. **134**, 18804 (2012).

[22] B. J. Knurr and J. M. Weber, J. Phys. Chem. A **118**, 4056 (2014).

[23] B. J. Knurr and J. M. Weber, J. Phys. Chem. A **118**, 8753 (2014).

[24] G. B. S. Miller, T. K. Esser, H. Knorke, S. Gewinner, W. Schoellkopf, N. Heine, K. R. Asmis, and E. Uggerud, Angew. Chem. Int. Ed. **53**, 14407 (2014).

[25] R. S. Walters, N. R. Brinkmann, H. F. Schaefer, and M. A. Duncan, J. Phys. Chem. A **107**, 7396 (2003).

[26] G. Gregoire and M. A. Duncan, J. Chem. Phys. **117**, 2120 (2002).

[27] G. Gregoire, N. R. Brinkmann, D. van Heijnsbergen, H. F. Schaefer, and M. A. Duncan, J. Phys. Chem. A **107**, 218 (2003).

[28] N. R. Walker, R. S. Walters, G. A. Grieves, and M. A. Duncan, J. Chem. Phys. **121**, 10498 (2004).

[29] J. B. Jaeger, T. D. Jaeger, N. R. Brinkmann, H. F. Schaefer, and M. A. Duncan, Can. J. Chem. **82**, 934 (2004).

[30] N. R. Walker, R. S. Walters, and M. A. Duncan, J. Chem. Phys. **120**, 10037 (2004).

[31] A. M. Ricks, A. D. Brathwaite, and M. A. Duncan, J. Phys. Chem. A **117**, 11490 (2013).

[32] A. Iskra, A. S. Gentleman, A. Kartouzian, M. J. Kent, A. P. Sharp, and S. R. Mackenzie, J. Phys. Chem. A **121**, 133 (2017).

[33] H. Xie, J. Wang, Z. Qin, L. Shi, Z. Tang, and X. Xing, J. Phys. Chem. A **118**, 9380 (2014).

[34] M. J. Frisch, G. W. Trucks, H. B. Schlegel, G. E. Scuseria, M. A. Robb, J. R. Cheeseman, G. Scalmani, V. Barone, B. Mennucci, G. A. Petersson, H. Nakatsuji, M. Caricato, X. Li, H. P. Hratchian, A. F. Izmaylov, J. Bloino, G. Zheng, J. L. Sonnenberg, M. Hada, M. Ehara, K. Toyota, R. Fukuda, J. Hasegawa, M. Ishida, T. Nakajima, Y. Honda, O. Kitao, H. Nakai, T. Vreven, J. J. A. Montgomery, J. E. Peralta, F. Ogliaro, M. Bearpark, J. J. Heyd, E. Brothers, K. N. Kudin, V. N. Staroverov, T. Keith, R. Kobayashi, J. Normand, K. Raghavachari, A. Rendell, J. C. Burant, S. S. Iyengar, J. Tomasi, M. Cossi, N. Rega, J. M. Millam, M. Klene, J. E. Knox, J. B. Cross, V. Bakken, C. Adamo, J. Jaramillo, R. Gomperts, R. E. Stratmann, O. Yazyev, A. J. Austin, R. Cammi, C. Pomelli, J. W. Ochterski, R. L. Martin, K. Morokuma, V. G. Zakrzewski, G. A. Voth, P. Salvador, J. J. Dannenberg, S. Dapprich, A. D. Daniels, O. Farkas, J. B. Foresman, J. V. Ortiz, J. Cioslowski, and D. J. Fox, *Gaussian 09, Revision D.01*, Wallingford CT: Gaussian Inc., (2013).

[35] Z. Zhao, X. Kong, D. Yang, Q. Yuan, H. Xie, H. Fan, J. Zhao, and L. Jiang, J. Phys. Chem. A **121**, 3220 (2017).